Investigation of Surface Quality in High Speed Welding of Aluminum Using Adjustable Ring-mode Fiber Laser

M. R. Maina, Y. Okamoto, M. Närhi, J. Kangastupa, J. Vihinen and A. Okada

***Abstract*—**Sheet metals joint technology is highly required in many manufacturing industries where aluminum finds great application. Laser welding of aluminum has difficulties due to its low melting point, high thermal conductivity and low absorptivity. Upon reaching the melting point, the absorptivity increases with increasing temperature. In deep penetration welding, a lot of spatter arise hence deterioration of surface quality, while good surface quality is an essential factor to improve component functionality. In order to achieve deep penetration with stable welding phenomenon and ensure good surface quality, at a high welding speed, adjustable ring-mode fiber laser has been employed, since it offers high power with a dynamic adjustable beam profile consisting of a center part and a ring-part. Pure-ring-mode irradiation using ring power only and dual-mode irradiation using both center power and ring power, were investigated through experiments and numerical simulations. Dual-mode irradiation made it possible to stabilize the welding process. The center power helps to achieve sufficient deep penetration, while ring power ensures good temperature distribution.

***Keywords*—**Adjustable ring-mode fiber laser, Aluminum, Laser welding, Surface quality.

I. INTRODUCTION

LASER welding technology has been used in many industries because of its high accuracy and efficiency. In comparison with conventional welding processes, laser welding offers the benefits of precision control of heat input, minimum thermal distortion, and small heat affected zones (HAZ) and excellent repeatability [1]. In addition, deep penetration welding capability of lasers makes it possible to weld thick metal sheets and also offers a great potential in joining of materials such as aluminum.

In this study, a non-heat treatable, Al-Mg alloy 5022 GC45-O was used. The addition of magnesium to aluminum increases strength through solid solution strengthening and improves their strain hardening ability. Recent application technologies of aluminum to automobiles have shown that aluminum alloy 5022 finds great application in vehicle body panels, since it is a high-strength, high-formability and light weight material [2]. These applications demand for an efficient and high speed method of joining aluminum metal sheets, with the aim of achieving good surface quality and high productivity.

There is a limit to which welding speeds can be increased without affecting the weld bead quality. The humping phenomenon sets a limit to the processing speed in laser beam welding for a given laser beam intensity. In order to show humps formation at high welding speeds, Fabbro and Amara developed a 3-D transient model based on numerical resolution of the fluid flow and heat transfer equations for deep penetration laser welding at high welding speed condition, which resulted in humping phenomenon [3]. When this phenomenon occurs, the height of the weld bead varies with the welding speed [4]. For a given configuration of material and processing parameters, there arises melt pool instability upon exceeding a certain welding speed. Thomy et al., through numerical and experimental investigations using a single-mode fiber laser, have reported that at a high welding speed, melt flow around the keyhole may result in a stagnation area behind the keyhole, destabilizing the melt pool surface. This promotes the onset of humping, which is characterized by formation of periodic droplets and severe undercuts on the weld bead surface [5].

The prerequisite for the onset of humping is an upward oriented melt pool stream due to drag forces. The higher the speed, the smaller the inclination angle of the absorption front, thus the upward momentum of the melt pool increases. The smaller the focus diameter, the shorter the humping length. The drag forces are reduced as the evaporation pressure at the absorption front decreases with lower intensity [6].

Laser welding of aluminum has difficulties due to its low melting point, high reflectivity and high thermal conductivity. The ideal situation for laser welding is to have materials with high absorptivity and low thermal conductivity. Normally, the absorptivity varies depending on the temperature; as a material becomes hot, the absorptivity increases. For aluminum, upon reaching the melting point, the absorptivity increases with increasing temperature and the process becomes unstable. A lot of spatter arise, and deep penetration welding with good surface quality becomes a challenge. In addition, at high welding

M. R. Maina, Nontraditional Machining Laboratory, Okayama University, Japan (phone: +819022901655; fax: +81862518039; e-mail: maina@ntmlab.mech.okayama-u.ac.jp).
Y. Okamoto, Nontraditional Machining Laboratory, Okayama University, Japan (e-mail: Yasuhiro.Okamoto@okayama-u.ac.jp).
M. Närhi, Corelase Oy, Finland (e-mail: matti.narhi@corelase.fi)
J. Kangastupa, Corelase Oy, Finland (e-mail: jarno.kangastupa@corelase.fi)
J. Vihinen, Laser Application Laboratory, Tampere University of Technology, Finland (e-mail: jorma.vihinen@tut.fi)
A. Okada, Nontraditional Machining Laboratory, Okayama University, Japan (e-mail: okada@ntmlab.mech.okayama-u.ac.jp)

speeds, the humping phenomenon leads to deterioration of the surface quality.

There is need for deep penetration welding, and also maintenance of good surface quality for the various applications of aluminum, in order to enhance component functionality. Nakashiba et al. have shown that, for good surface quality, boundary region between keyhole and heat conduction welding mode would have advantages, but stabilization of the welding phenomenon is important [7].

Recently, the advancements of laser technologies have led to availability of lasers with high power and high beam quality, such as adjustable ring-mode (ARM) fiber lasers. ARM fiber laser is suitable for wide range of materials and thicknesses. It offers a dynamic adjustable beam profile with two parts namely; center part and ring part, hence a unique form of intensity distribution.

To achieve deep penetration with stable absorption and ensure good surface quality, at a high welding speed, ARM fiber laser has been employed. There is possibility to perform superior temperature distribution by combination of center power and ring power. Therefore, laser welding of aluminum, using ARM fiber laser, was investigated experimentally and numerically using a finite element method (FEM) based model. The influence of laser intensity distribution on the weld bead was discussed.

II. EXPERIMENTAL METHOD

Overlap welding of two aluminum alloy 5022 sheets, each 1.5 mm thick, was performed at a welding velocity of 15 m/min. The processing head was fixed, while the specimen was moved. The back side of the sheets was left open to air. The processing head employed concave mirrors with a collimation of 100 mm and a focal length of 150 mm. The laser wavelength was 1070 nm, and the beam spot diameters for the outer ring and center were 270 μm and 105 μm, respectively. The fiber used in this study had an inner core diameter of 70 μm, an outer core diameter of 180 μm and a gap of 15 μm, as shown in Fig. 1. The gap is filled with a glass material of low refractive index. Fig. 2 shows the intensity distributions for dual-mode and pure-ring-mode operations. The beam parameter products for the center and ring part were 2 mm·mrad and 8 mm·mrad, respectively.

Nitrogen was used as the shielding gas. It was supplied from the backside, at a flow rate of 15 L/min, through an off-axial nozzle of size 7.0 ×1.5 mm, inclined at an angle of 45° to the vertical. The gap between the off-axial nozzle tip and the workpiece surface was set at 10 mm. The experimental setup is schematically shown in Fig. 3. Table 1 shows the combinations of laser center power and ring power used in this study.

Weld bead evaluation involved measurements of bead width and height, roughness measurement, evaluation of surface appearance, and observation of cross-section. A laser displacement sensor (LDS) with a repeatability of 0.2 μm was used for weld bead profile measurement as shown in Fig. 4. Weld bead surfaces were observed using an optical microscope. Measurement of roughness involved use of stylus type roughness measurement machine with a stylus radius of 2 μm. For cross-section observation, the surface was first polished and then etched using HCl with 35% weight concentration.

TABLE 1
LASER POWER COMBINATIONS.

Case	Center power P_c (kW)	Ring power P_r (kW)	Total power (kW)
A	0	5.0	5.0
B	1.5	3.5	5.0

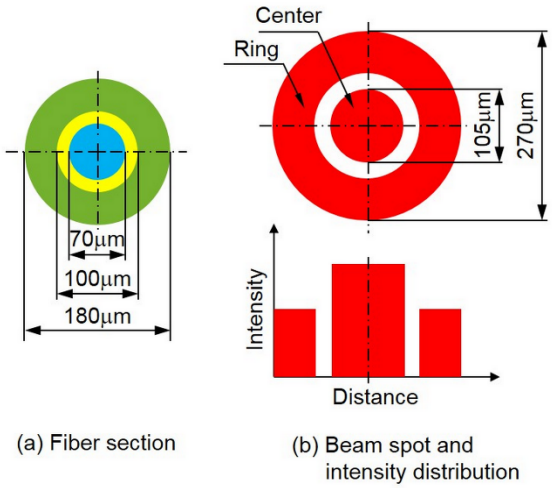

Fig. 1 Schematic illustration of fiber section, beam spot and intensity distribution.

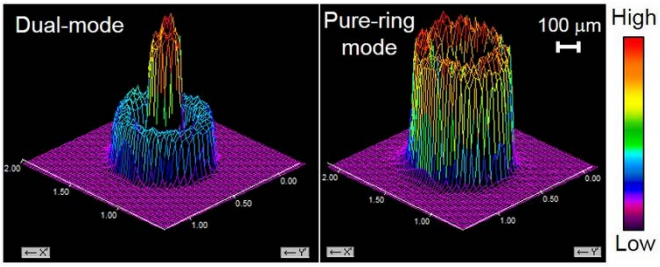

Fig. 2 Intensity distributions for dual-mode and pure-ring-mode operations.

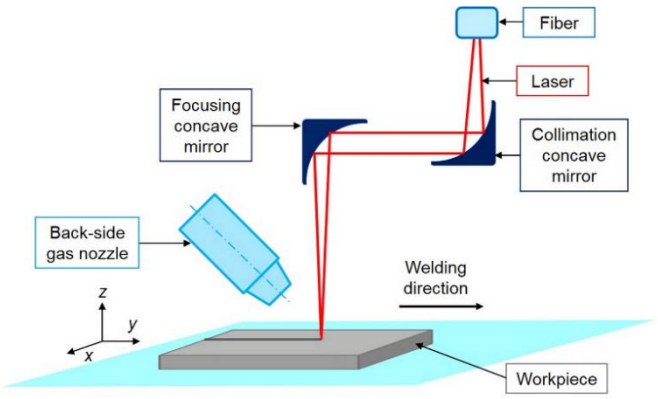

Fig. 3. Schematic illustration of experimental setup.

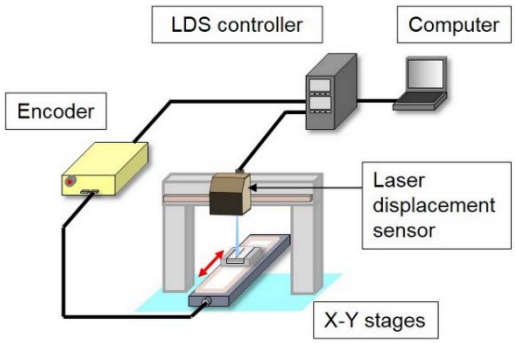

Fig. 4 Setup for weld bead profile measurement using laser displacement sensor.

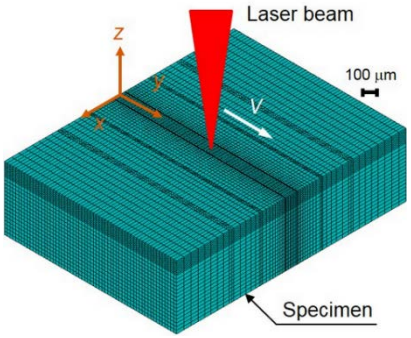

Fig. 5 FEM model for laser welding process.

III. NUMERICAL ANALYSIS METHOD

To further study the welding phenomenon in welding of aluminum using ARM laser, numerical simulation was performed using the general finite element program 'ANSYS'. Center and ring power combinations similar to experimental work were used. The geometry model employed similar total thickness of 3 mm as the experimental work. However, a small section of 8 mm length and 6 mm width was chosen. The transient temperature distribution of the welded specimen was a function of time *t* and Cartesian coordinate system with *y*-axis along the welding direction, *z*-axis along the thickness direction, and the origin located on the specimen surface as shown in Fig. 5. The governing equation for the transient heat conduction can be written as:

$$\rho c \frac{\partial T}{\partial t} = k\left(\frac{\partial^2 T}{\partial x^2} + \frac{\partial^2 T}{\partial y^2} + \frac{\partial^2 T}{\partial z^2}\right) + Q_i \quad (1)$$

where, T is the temperature, ρ the material density, c the specific heat, k the thermal conductivity, and Q_i the internal heat generation per unit volume.

The temperature dependent material properties are important for the accurate calculation of temperature field. The temperature response in a material involved in high heat fluxes is determined by thermal material properties of thermal conductivity, specific heat and density, which are dependent on temperatures [8]. Enthalpy values around the fusion and vaporization regions were computed in order to take into consideration the latent heat of aluminum. Aluminum has a melting point of 933 K and an evaporation point of 2741 K.

The welding process was performed in the middle of the specimen. Meshes were graded such that they were finest in the region of highest and most rapid temperature gradient near the heat input. Course meshes were used for the regions farthest from the heating zones. In addition, element sizes increased across the thickness of the specimen, being finer near the heated side of the specimen. The initial condition for the entire region was set at a room temperature of 293 K. The heat flux generated by the laser beam was applied on the top surface of the specimen. For the non-irradiated top surface and *x*-*z* end planes, the heat flux was assumed to be convective with a heat transfer coefficient of 10 W/(m²·K), while *y*-*z* end planes had infinite boundary temperature. The heat source was moved along *y*-axis in steps of 0.08 ms at a scanning velocity of 250 mm/s, with beam spot diameters of 270 µm in the outer ring and 105 µm at the center.

The absorption rate of a material is related to the material resistivity and the wavelength of the laser irradiation. However, absorptivity increases with increase in keyhole depth. Surface absorptivity is affected by mechanisms related to surface geometry during keyhole generation, through creation of surface ripples, which enhances absorptivity [9]. In this study, the absorptivity of aluminum at the top surface was taken to be 0.2 from literature [10], but increased gradually with heat input across the thickness. The FEM model used a combination of surface heat source and volumetric heat source. The total heat input was computed from the summation of surface heat source on the top surface and the volumetric heat source along the thickness direction as shown in equation 2.

$$Q = Q_s + Q_v \quad (2)$$

where Q is total heat input, Q_s surface heat flux, and Q_v volumetric heat flux. It was assumed that 25% of the heat power was absorbed on the surface of the specimen and the remaining 75% was absorbed by the keyhole wall. The surface heat flux was applied in top-hat mode, while the volumetric heat flux was applied in Gaussian distribution as expressed by equations 3 and 4, respectively.

$$Q_s = P_s/(\pi R^2) \quad (3)$$

$$Q_v = \frac{3P_v}{\pi {r_0}^2 h_d} exp\left(-3\frac{{r_c}^2}{{r_0}^2}\right)\cdot\left(1-\frac{z_i}{h_d}\right) \quad (4)$$

where R is beam spot radius, P_s power absorbed on the surface, P_v power absorbed by keyhole wall, r_0 initial radius of keyhole, h_d maximum keyhole depth, r_c current keyhole radius, and z_i current keyhole depth.

IV. RESULTS AND DISCUSSION

A. *Effects of laser power density on weld bead*

Fig. 6 shows weld bead surface and cross-section appearances by using different intensity distributions under the same total power condition, while Fig. 7 shows the

corresponding bar graph for variations of weld bead height, penetration depth and surface roughness. Both cases of pure-ring-mode, where only ring power is used, and dual-mode, where both center power and ring power are used, showed almost equal penetration depths at the same total power of 5.0 kW. However, weld bead roughness was considerably higher in the case of pure-ring-mode. Center power helps to initiate faster keyhole formation and a small keyhole diameter is expected. This helps to reduce spattering and prevent humping, hence reduction in surface roughness of weld bead. However, too much center power may lead to high material removal, hence deterioration of the weld bead.

The cross-sectional profile of the weld bead for dual-mode welding presents an 'hourglass' shape, which means that the top is the widest, the bottom narrower, and the middle the narrowest. This can be explained by influence of surface tension gradients in the molten metal flow. The maximum flow velocity of molten metal appears on the surface of melt pool, where there is the maximum temperature gradient. The molten metal flows from the higher-temperature keyhole boundary at the center of the beam to the lower temperature melt pool boundary. This leads to an expansion of the fusion zone in the top and bottom surface areas. For pure-ring-mode welding, since only ring power is present, a larger keyhole diameter is expected, and thus

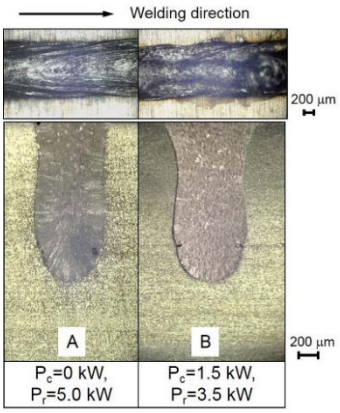

Fig. 6 Surface and cross-section appearance under different power densities.

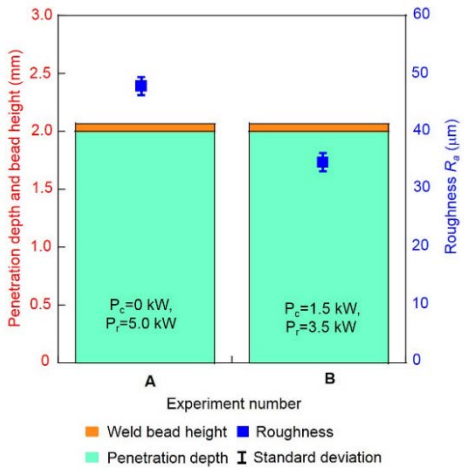

Fig. 7 Variation of weld bead height, penetration depth and surface roughness under different power densities.

the surface tension gradients in the molten metal flow is low. It is considered that heat is uniformly distributed around the ring, hence the uniform profile.

B. Influence of temperature distribution

The weld bead profiles obtained from experiments and simulations, under similar laser processing parameters, were compared in order to verify the simulation results. The simulation results gave a good estimation of the weld bead cross-section. Fig. 8 shows the temperature distribution isotherms on the top surface for dual-mode and pure-ring-mode cases where 5.0 kW total power was used in each case. The red part represents the molten and evaporated material at the center for temperatures above the melting point 933 K. The weld pool shapes around the high-energy heat source appear different. The 'tail' in dual mode case presents a bigger radius than that in pure ring mode case. The 'tail' shows the behavior of heat flow as the heat source moves along the surface. Dual mode case leads to a slower cooling rate compared to that of pure ring mode case.

Center power leads to faster keyhole formation thereby enhancing deep penetration. With sufficient keyhole, spattering is reduced and there is stability of the surface state of molten metal. A smaller keyhole diameter in dual mode case means that the melt pool region between the keyhole and the solid material is wider leading to a smooth flow. On the contrary, for pure ring mode, there is a larger keyhole diameter and the keyhole depth is smaller as shown in Fig. 9.

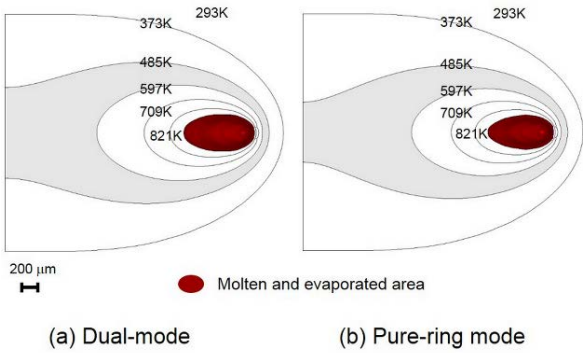

Fig. 8 Temperature distribution isotherms on the top surface for dual-mode and pure-ring-mode welding.

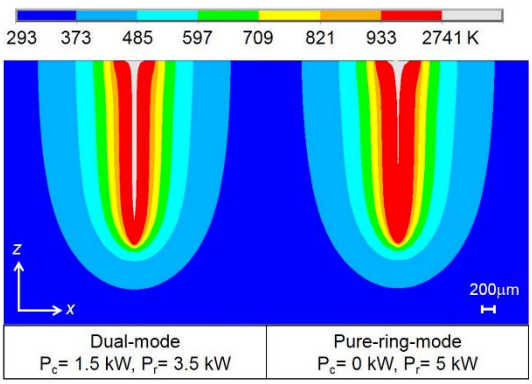

Fig. 9 Variations of keyholes for dual-mode and pure-ring-mode welding.

Despite having a smaller keyhole depth for pure-ring-mode welding, deep penetration could be achieved due to high power density at the ring. The temperature of the melt pool near the evaporated area was very high, being at the liquid-vapor transition region. From this study, dual-mode welding with high power ARM fiber laser has shown the capability of obtaining good surface quality and sufficient deep penetration, at high welding speeds.

V. CONCLUSIONS

Laser welding using adjustable ring-mode fiber laser proves to be a reliable high speed joining method for aluminum with the possibility of obtaining high quality welds. The main conclusions obtained in this study are as follows:

1) Dual-mode welding leads to a weld bead with lower surface roughness compared to pure-ring-mode welding.
2) Center power helps to initiate faster and sufficient keyhole formation, while ring power ensures good temperature distribution, hence stabilizing the welding process.

ACKNOWLEDGEMENT

The research work covered in this paper was partly supported by Japanese Ministry of Education, Culture, Sports, Science and Technology, and Jomo Kenyatta University of Agriculture and Technology, Kenya.

REFERENCES

[1] S. Josefine, C. Isabelle, and F. Alexander, “Laser welding process – a review of keyhole welding modelling,” Physics Procedia, vol. 78, pp. 182-191, 2015.
[2] I. Takashi, T. Kenji, Y. Hiroyuki, T. Yoshiki, and I. Tadayuki, “Wrought aluminum technologies for automobiles,” Kobelco Technology Review, vol. 26, pp. 55-62, 2005.
[3] R. Fabbro and E. Amara, “Modeling of humps formation during deep-penetration laser welding,” Applied Physics A: Materials Science and Processing, vol. 101, pp. 111-116, 2010.
[4] G. Hongping and S. Boris, “A practical use of humping effect in laser beam welding,” Journal of Laser Applications, vol. 23, pp. 012001, 2011
[5] C. Thomy, T. Seefeld, and F. Vollertsen, “Humping effect in welding of steel with single-mode fibre laser,” Welding in the World, vol. 52, pp. 9-18, 2008.
[6] O. Andreas, A. Patschger, and S. Michael, “Numerical and experimental investigations of humping phenomena in laser micro welding,” Physics Procedia, vol. 83, pp. 1415-1423, 2016.
[7] S. Nakashiba, Y. Okamoto, T. Sakagawa, M. Harada, and A. Okada, “The boundary of keyhole generation in micro-welding of aluminum alloy by pulsed Nd:YAG laser with superposition of continuous diode laser,” Journal of the Japan Society for Precision Engineering, vol. 80, pp. 419-424, 2014.
[8] N. Kethireddy, S. Ammiraju, G. Kalvala, and G. Nallacheruvu, “Temperature dependence of density and thermal expansion of wrought aluminum alloys 7041, 7075 and 7095 by gamma ray attenuation method,” Journal of Modern Physics, vol. 4, pp. 331-336, 2013.
[9] R. Fabbro, F. Coste, S. Slimani, and F. Briand, “Study of keyhole behaviour for full penetration Nd:YAG CW laser welding,” J. Phys. D: Appl. Phys., vol. 38, pp. 1881-1887, 2005.
[10] T. Forsman, A. Kaplan, J. Powell, and C. Magnusson, “Nd:YAG laser welding of aluminium; factors affecting absorptivity,” Lasers in Engineering, vol. 8, pp. 295-309, 1999.